

An annealing study of an oxygen vacancy related defect in SrTiO₃ substrates

M. E. Zvanut, S. Jeddy, E. Towett, G. M. Janowski, C. Brooks, and D. Schlom

Citation: *Journal of Applied Physics* **104**, 064122 (2008); doi: 10.1063/1.2986244

View online: <http://dx.doi.org/10.1063/1.2986244>

View Table of Contents: <http://scitation.aip.org/content/aip/journal/jap/104/6?ver=pdfcov>

Published by the [AIP Publishing](#)

Articles you may be interested in

[Oxygen vacancies induced switchable and nonswitchable photovoltaic effects in Ag/Bi_{0.9}La_{0.1}FeO₃/La_{0.7}Sr_{0.3}MnO₃ sandwiched capacitors](#)

Appl. Phys. Lett. **104**, 031906 (2014); 10.1063/1.4862793

[The annealing mechanism of the radiation-induced vacancy-oxygen defect in silicon](#)

J. Appl. Phys. **111**, 113530 (2012); 10.1063/1.4729323

[Iron-related defect levels in SrTiO₃ measured by photoelectron paramagnetic resonance spectroscopy](#)

J. Appl. Phys. **107**, 083513 (2010); 10.1063/1.3372760

[Electron spin resonance investigation of oxygen-vacancy-related defects in Ba Ti O₃ thin films](#)

Appl. Phys. Lett. **87**, 022903 (2005); 10.1063/1.1954900

[Oxygen vacancy mobility determined from current measurements in thin Ba_{0.5}Sr_{0.5}TiO₃ films](#)

Appl. Phys. Lett. **73**, 175 (1998); 10.1063/1.121746

MIT LINCOLN
LABORATORY
CAREERS

Discover the satisfaction of
innovation and service
to the nation

- Space Control
- Air & Missile Defense
- Communications Systems & Cyber Security
- Intelligence, Surveillance and Reconnaissance Systems
- Advanced Electronics
- Tactical Systems
- Homeland Protection
- Air Traffic Control

 **LINCOLN LABORATORY**
MASSACHUSETTS INSTITUTE OF TECHNOLOGY



LEARN MORE

An annealing study of an oxygen vacancy related defect in SrTiO₃ substrates

M. E. Zvanut,^{1,a)} S. Jeddy,¹ E. Towett,^{1,b)} G. M. Janowski,² C. Brooks,³ and D. Schlom³

¹Department of Physics, University of Alabama at Birmingham, Birmingham, Alabama 35294-1170, USA

²Department of Materials Science and Engineering, University of Alabama at Birmingham, Birmingham, Alabama 35294-1170, USA

³Department of Materials Science and Engineering, Pennsylvania State University, University Park, Pennsylvania 16802, USA

(Received 12 May 2008; accepted 3 August 2008; published online 29 September 2008)

The study addresses the stability of point defects in SrTiO₃ (STO) during thin film processing using electron paramagnetic resonance (EPR) spectroscopy. In particular, the intensity of the Fe³⁺V_O EPR signal is monitored after various steps during the growth of STO films on STO substrates. Controlled O₂ and vacuum heat treatments are also performed to clarify the fundamental mechanisms responsible for the effects of different processing steps. Comparison of results from film fabrication with those obtained during exposure to the control ambient shows that the presence of oxygen in the pretreatment growth atmosphere decreases the amount of the Fe³⁺V_O complex, but exposure to the low pressure environment of the growth chamber returns the signal to the original intensity. These results are consistent with accepted theories of oxygen vacancy diffusion. However, an unexpected decrease in the oxygen vacancy related signal is also observed during vacuum treatment of an as-received sample. Furthermore, the decrease occurs over the same temperature range as seen for an O₂ anneal. The difference between the O₂ and vacuum treatments is revealed in postannealing photoinduced EPR and resistivity measurements, which indicate that vacancy related centers change charge state during the O₂ anneal and are not removed by oxygen. The effect of the vacuum treatment, though different from that of oxygen, is not yet clear as no charge state changes were induced after exposure to visible or ultraviolet radiation, but the conductivity of the samples changed. © 2008 American Institute of Physics. [DOI: 10.1063/1.2986244]

I. INTRODUCTION

SrTiO₃ (STO) and related oxide compounds have long been utilized in ferroelectric systems for microwave applications because of their high dielectric constant. More recently, thin films of STO are studied as potential candidates for multiferroic devices and as the oxide layer of electronic memories.^{1–3} For both systems, bulk STO often serves as a substrate for the overlying oxide film.^{1–3} Common to all of the applications of STO are concerns about the well-known instability of oxygen and the reported influence of oxygen vacancies and other defects on conductivity and optical processes.^{3–7}

STO is a cubic perovskite where every Sr is surrounded by 12 oxygen atoms and every Ti is surrounded by 6 oxygen atoms. If one pictures the charge exchange as ionic, Sr may be thought of as Sr²⁺, Ti as Ti⁴⁺, and O as O²⁻. Transition metals such as Fe, Mn, and Cr often substitute for Ti and assume the charge states Fe³⁺, Mn²⁺, and Cr³⁺. When one of the six oxygen atoms surrounding the impurity is missing, the complex is referred to as Xⁿ⁺V_O, where X can be one of several transition metals and “n” represents the charge state. Optical absorption measurements have been used to predict

the existence of impurities and defect complexes, and magnetic resonance measurements support these claims.^{8–15}

Numerous electrical, magnetic resonance, and optical studies have addressed the stability of oxygen vacancies and their relationship with electrical conductivity.^{6,7,13–16} For example, the well-known reversibility of the conductivity when STO is exposed to vacuum and ambient O₂ is sometimes associated with oxygen vacancy related species.^{6,7} The stability of the oxygen vacancy complex in STO was thoroughly studied using *in situ* electron paramagnetic resonance (EPR)/annealing measurements at temperatures between 170 and 540 K.¹⁶ Using 0.02%–0.3% Fe-doped samples, Merkle and Maier¹⁶ concluded that the presence of Fe³⁺V_O can reduce conductivity at temperatures of up to 200 °C, but the effects depend strongly on doping. Despite all of these studies, diffusion of the oxygen vacancy remains controversial. Furthermore, in a practical context, none of the studies address the specific ambient conditions typically used in film growth.

Here, we address the effects of film growth on the stability of selected point defects in bulk STO. Specifically we monitor three defect centers, one involving an oxygen vacancy, during different stages of deposition of a STO film on a commercially grown STO substrate. The concentration of the same centers is also measured during controlled heat treatment experiments in oxygen and ambient vacuum. Combined with postannealing optical excitation, the results indi-

^{a)}Electronic mail: mezvanut@uab.edu.

^{b)}Present address: Engineering Technology Department, Grambling State University, Grambling, LA 71245, USA.

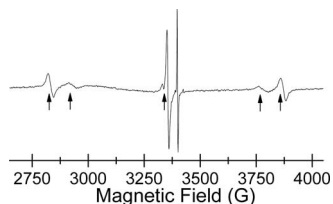


FIG. 1. EPR spectrum of a STO substrate obtained at room temperature with the magnetic field parallel to a (001) axis. The five arrows point to the Fe^{3+} impurity spectrum. The sharp line to the right of the Fe^{3+} central line is Cr^{3+} . The small barely resolved line to the left is one of the three lines of $\text{Fe}^{3+}\text{V}_\text{O}$.

cate that oxygen treatment primarily alters the electrical charge state of the vacancy, while exposure to vacuum causes different changes, either conversion to a different charge state or creation of the vacancy.

II. EXPERIMENTAL DETAILS

STO substrates from two different vendors were used for this study. Most were grown by the Vernuil method, but some studies were performed on samples grown using the float zone technique. The (001) oriented substrates were cut into $0.24 \times 1 \text{ cm}^2$ pieces for EPR measurements. Controlled heat treatments were performed in either dry O_2 ($\text{H}_2\text{O} < 1 \text{ ppm}$) or vacuum (10^{-5} Torr) over the temperature range of 200–800 °C. The moisture content of the gas was measured at the exit port of the furnace tube; the pressure and temperature during the vacuum anneals were measured at the sample. Samples were also subjected to the processing steps used for the deposition of a STO film. In this case, the as-received samples were first rinsed in hydrofluoric acid (HF) for 30 s at room temperature (step 1), then annealed in 1 atm O_2 at 950 °C for 2 h, and cooled to room temperature in O_2 (step 2).¹⁷ The samples were loaded into the sample chamber and heated to 650 °C in $5 \times 10^{-7} \text{ Torr}$ vacuum with 10% O_3 for 1 h (step 3). Finally, the preceding step was repeated with the shutters open so that a 40 nm thick STO film was grown (step 4). EPR was measured on the as-grown samples and after each step of the processing sequence.

EPR spectroscopy was performed at room temperature using a 10 GHz spectrometer. The only defects seen in all of these substrates were those common to STO. Two are isolated impurities substituting for the Ti^{4+} ion, Fe^{3+} and Cr^{3+} . The other is a defect complex consisting of substitutional iron with nearest neighbor oxygen vacancy, $\text{Fe}^{3+}\text{V}_\text{O}$. The well-studied defects were identified using standard EPR spectral analysis as described in many texts.¹⁸ A spectrum illustrating these three EPR centers is shown in Fig. 1, where the arrows point to the five lines of the electron spin 5/2 Fe^{3+} impurity. The sharp line immediately to the right of the central line of Fe^{3+} is Cr^{3+} . The small, barely resolved line to the left is one of the three EPR signal due to $\text{Fe}^{3+}\text{V}_\text{O}$. Separate spectra taken under conditions that optimize the detection of each of these centers were used when monitoring the relative and total intensities. Measurements at 77 K revealed the more complicated spectra of the defects in the reduced symmetry environment, as expected. However, no additional defects were identified. The defect concentrations were ob-

tained by comparison of the EPR signal with that of a pitch standard, assuming a uniform distribution of centers. In one of the two samples used for the processing dependence study, the concentrations of Fe^{3+} and Cr^{3+} were 3×10^{16} and $2 \times 10^{14} \text{ cm}^{-3}$, respectively (hereafter referred to as sample 1). The amounts in the other sample (sample 2) were $7 \times 10^{16} \text{ cm}^{-3}$ (Fe^{3+}) and $2 \times 10^{15} \text{ cm}^{-3}$ (Cr^{3+}). The absolute concentration of the defect complex is not easily assessed due to the angular dependent intensity. However, relative concentration measurements show that sample 2 had approximately three times the number of $\text{Fe}^{3+}\text{V}_\text{O}$ centers seen in sample 1. The amount of each defect in the samples used for the controlled annealing studies ranged from that observed in sample 2 to an order of magnitude larger. The annealing results presented here were the same in all samples, independent of the initial defect concentration.

To avoid errors inherent in estimating the total defect concentration, the amount of centers relative to that in the untreated sample, rather than total amount, is reported after each processing step or anneal. The relative number of defects was obtained from comparison of the EPR peak-to-peak signal intensities of the as-received and annealed samples. For the $\text{Fe}^{3+}\text{V}_\text{O}$ complex, the sample was rotated so that the highly angular dependent signal always occurred at the same magnetic field position, after normalization to frequency. This process ensured that any signal intensity changes were caused by the heat treatment and were not due to the angular dependent intensity variation. Independent studies showed that Cr^{3+} is sensitive to room light, so the samples were routinely kept in the dark for about 24 h after the anneal and before measurement. All samples were mounted in identical holders throughout the study to minimize variations in the sample position in the cavity.

The EPR signal represents a specific charge state of a defect. Therefore illumination that places the defect in an excited or ionized state may alter the intensity of the EPR signal. Samples were illuminated with a 400 nm 5 mW light emitting diode (LED) to test for such effects. Typically, a sample was exposed to light for 10 min prior to EPR measurement, and the illumination was continued while acquiring the spectrum.

The resistivity of some of the samples was measured using pressed In contacts and two-point probe current-voltage (I - V) measurements. As expected, the conductivity of the as-grown and O_2 annealed samples was so low that the contact resistance dominated and the I - V curves were extremely nonlinear. However, the vacuum annealed samples produced linear I - V characteristics with resistivity ρ on the order of $10^6 \Omega \text{ cm}$. The value is higher than is typically measured for vacuum annealed substrates because the samples were left at room temperature in air for several weeks before the I - V measurements were made.¹⁹

III. RESULTS AND DISCUSSION

An EPR spectrum of the oxygen vacancy complex measured in sample 2 before any heat treatment is shown in spectrum (a) in Fig. 2. Spectra (b)–(e) were obtained after each step of the processing sequence, where (b) was mea-

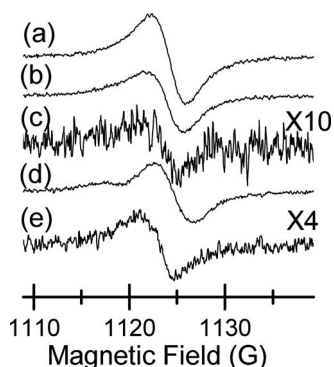


FIG. 2. EPR spectra of $\text{Fe}^{3+}\text{V}_\text{O}$ measured on a STO substrate: (a) as grown, (b) after HF etch, (c) after predeposition O_2 treatment, (d) after simulated deposition, and (e) after deposition of STO film.

sured after etching in HF, (c) after a preparation anneal in O_2 , (d) after exposure of the sample to growth conditions without film deposition, and (e) after film deposition. Similar results were obtained for the other sample except for the deposition of the film, which left the $\text{Fe}^{3+}\text{V}_\text{O}$ signal unchanged. The intensities of the Fe^{3+} and Cr^{3+} signals followed similar trends as the vacancy complex. Spectrum (b) in Fig. 2 shows that the HF treatment produced no change in the spectra, supporting the notion that the acid clean primarily attacks the surface. EPR detects the total number of defects throughout the bulk of a material. Thus, assuming a uniform distribution of centers, a change in the surface concentration will not necessarily be sensed by the spectrometer. Step 3, involving O_2 , decreases the oxygen vacancy complex by at least a factor of 10. Step 4, which occurred at high vacuum, returns the oxygen vacancy complex to approximately its initial concentration. Note that the data indicate that the O_3 added during the deposition step did not prevent changes in vacancy related concentration as might be expected. Step 5, the deposition of the film, reduced the signal by no more than a factor of 4. More significantly, the final growth conditions had different effects on the two samples, suggesting that interaction of the substrate with various gasses in the processing ambient may depend critically on the method of substrate growth. However, much more thorough studies need to be completed before such a generalization can be made.

To better understand the effect of processing conditions on the substrate, several controlled annealing experiments were performed without the additive features of processing steps such as using silver paint to mount the sample or adding ozone to the vacuum system. In the first, samples were subjected to isochronal heat treatments in dry O_2 followed by a series of isochronal vacuum treatments at temperatures between 200 and 800 °C. The results provide the temperatures at which the defects are activated and/or quenched. The second experiment, in which an as-received sample was heat treated in 10^{-5} Torr vacuum, was designed to test the effects the predeposition O_2 fabrication step. Keeping in mind that all of the results presented in Figs. 2 and 3 may represent either charge state changes or vacancy annihilation, selected samples were exposed to ultraviolet radiation to investigate the possibility of charge transfer reactions.

Results from the first type of experiment are shown in

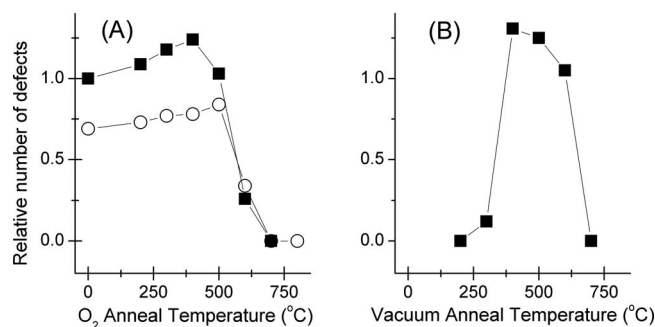


FIG. 3. EPR intensities of $\text{Fe}^{3+}\text{V}_\text{O}$ measured with respect to the intensity measured in sample 1 before annealing. (A) Filled squares: sample 1, O_2 anneal; unfilled circles: sample 2, vacuum anneal. (B) Filled squares: sample 1, subsequent vacuum anneal.

Fig. 3 as filled squares. A STO substrate was subjected to sequential 1 h heat treatments in O_2 up to a temperature of 700 °C followed by a series of 1 h treatments in vacuum. The filled squares in Fig. 3(a) represent the relative intensity of the $\text{Fe}^{3+}\text{V}_\text{O}$ EPR signal measured after each O_2 treatment and the filled squares in Fig. 3(b) were obtained during the subsequent vacuum anneal. The circles will be discussed later. The data show a sharp decrease at temperatures greater than 500 °C during the O_2 treatment and an increase between 300 and 400 °C during the vacuum anneal. While the data demonstrate that the effects of an O_2 pretreatment can be reversed, Fig. 3(b) shows that the reversal occurs within a window of only a few hundred centigrade degrees. More significantly, comparison of the thresholds in Figs. 3(a) and 3(b) show that the temperature required to revive the defect complexes in vacuum is 200–300 °C lower than that required to quench them in O_2 . Thus, a pretreatment in O_2 will be unstable if the sample is subsequently subjected to vacuum conditions at temperatures above 300 °C.

The second experiment involves annealing an as-received sample in vacuum to test the effects of the O_2 treatment performed before film deposition. The results of 1 h heat treatments of an as-received sample at 10^{-5} Torr are shown as the unfilled circles in Fig. 3(a). Two significant features should be noted from these data. First, the defect concentration in the as-received vacuum treated sample does not change at $T < 400$ °C, contrary to that observed for the oxidized vacuum annealed sample [Fig. 3(b)]. Thus, an as-received substrate should be stable in vacuum at sufficiently low temperature. Second, the graph highlights the unexpected similar temperature dependence for O_2 and vacuum anneals. This similarity extends to the isolated Fe^{3+} impurity (not shown). Significantly, chromium exhibits a different temperature dependence from that of the iron related species, affirming that the Fe^{3+} and $\text{Fe}^{3+}\text{V}_\text{O}$ trends are not an artifact of our annealing processes.

The EPR measurements were supplemented by resistivity and photoinduced EPR studies of several different vacuum and O_2 annealed samples. Lack of good Ohmic contacts for the unannealed samples prevented determination of the resistivity. But comparison with published values for undoped as-grown SrTiO_3 suggests that $\rho > 10^9 \Omega \text{ cm}$ at room temperature.¹⁹ The O_2 annealed samples also exhibited poor ohmicity, suggesting that the high resistivity remained after

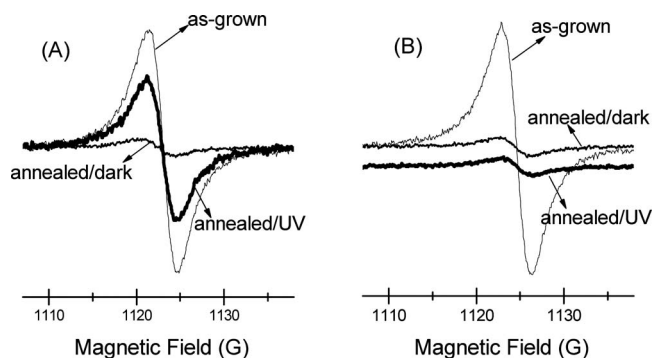


FIG. 4. EPR spectra of $\text{Fe}^{3+}\text{V}_\text{O}$ in as-grown samples (light weight). (A) Spectra measured after O_2 anneal: before illumination (medium weight) and after UV irradiation (heavy weight). (B) Spectra measured after vacuum anneal: before illumination (medium weight) and after UV irradiation (heavy weight). The UV spectrum in (B) is shifted vertically for clarity.

the oxygen anneals. I - V measurements of the vacuum treated samples yielded resistivities on the order of $10^6 \Omega \text{ cm}$. The significant decrease in resistivity after the vacuum anneal clearly distinguishes the vacuum and O_2 treated samples.

Illumination with ultraviolet light using a 5 mW LED also reveals a clear distinction between the two types of samples. While changes induced in Fe^{3+} and Cr^{3+} did not show a definitive trend with illumination, the $\text{Fe}^{3+}\text{V}_\text{O}$ intensity consistently increased after exposure to light for the O_2 treated samples and remained unchanged in the vacuum annealed samples. Figure 4 shows the spectra of an as-received sample (light solid line) and samples stepwise annealed to 700°C in O_2 or vacuum (medium-weight line). The heavy line illustrates the effects of UV irradiation on the two differently treated samples. Illumination of the O_2 treated samples returns the intensity of the $\text{Fe}^{3+}\text{V}_\text{O}$ spectra to within 60% of the preanneal value [heavy line, Fig. 4(a)], while the same exposure of a vacuum treated sample has no effect [heavy line, Fig. 4(b)]. Exposure of the vacuum treated samples at selected visible wavelengths down to 630 nm failed to induce the EPR signal of the vacancy complex.

As mentioned in Sec. I, EPR measurements are charge state specific. Therefore, changes in the EPR spectral intensity may reflect electronic ionization events rather than the physical motion of ions. In other words, the heat treatments may be altering the Fermi level E_F of the samples by means of thermally induced ionization processes, which changes the intensity of the $\text{Fe}^{3+}\text{V}_\text{O}$ center by capture or emission of an electron. Indeed, the Fe^{3+} and Cr^{3+} decreases seen in Fig. 3 must be due charge transfer because the temperatures used in the heat treatments are not expected to cause impurity diffusion but only electronic excitation. Below we discuss a possible interpretation for the O_2 and vacuum annealing data of $\text{Fe}^{3+}\text{V}_\text{O}$ in light of possible charge transfer reactions considering the conductivity and photoinduced EPR results.

The situation for the O_2 annealed samples may readily be explained by thermal ionization of the oxygen vacancy related center and impurities during heat treatment. Since the conductivity of the sample did not change within the limits of our measurement, we suggest that the centers oxidize by emitting an electron to a nearby defect, or perhaps to the O_2 gas itself. Once formed, the defects such as $\text{Fe}^{3+}\text{V}_\text{O}$ could be

returned to the 3+ state by ionization with UV light. If the thermally induced charge transfer processes caused the Fermi level to reach within kT ($T=300 \text{ K}$) of the valence band, one would expect room temperature conduction. However, according to the level scheme devised by Morin and Oliver,¹⁴ the Fe^{4+} energy is thought to be about 0.7 eV above the valence band edge. Since the Fermi level must be at or above this level for the existence of Fe^{4+} , E_F should be far enough from the band edge to make room temperature hole conduction negligible, consistent with the persistent high resistivity after annealing.

Interpretation of the vacuum anneal data is less clear because we were not able to revive the $\text{Fe}^{3+}\text{V}_\text{O}$ signal with UV light. One of two scenarios is possible. All of the defects may be directly ionized to the bands during the thermal treatment, accounting for the Cr^{3+} and Fe^{3+} changes observed in the EPR data and the measured conductivity change. The lack of photoresponse of the vacancy complex would be ascribed to a weak oscillator strength, placing stringent constraints on the photon energy and intensity needed for ionization. Alternatively, we suggest that the often suggested oxygen vacancy donor²⁰ created during vacuum annealing is responsible for the conductivity, and that the decrease in $\text{Fe}^{3+}\text{V}_\text{O}$ is due to capture of mobile oxygen.

In summary, we have shown that processing conditions involving O_2 at temperatures greater than 500°C can reduce the amount of the $\text{Fe}^{3+}\text{V}_\text{O}$ centers in a STO substrate by at least an order of magnitude. A subsequent vacuum treatment will reintroduce the vacancy complex at temperatures above 300°C , despite the presence of 10% O_3 in the ambient. Illumination with ultraviolet light shows that the changes induced by the O_2 treatment are electronic, rather than related to the motion of oxygen atoms. Exposure of as-grown substrates to vacuum at $T > 500^\circ\text{C}$ also decreases the $\text{Fe}^{3+}\text{V}_\text{O}$ concentration. In this case, ultraviolet light cannot reverse the effect. The mechanism for the decrease in the oxygen vacancy related centers is unclear. The signal intensity change is caused by either a charge state change or oxygen migration. In terms of the use of STO for thin film growth, the results indicate that treatment of as-received substrates at temperatures greater than 500°C in vacuum may alter the materials permanently, and treatment in O_2 over similar temperatures are unstable.

ACKNOWLEDGMENTS

The work at UAB was supported by the Office of Naval Research and the NSF/UAB ADVANCE program. E. Towett was supported by the NASA Alabama Space Grant Consortium Research Experiences for Undergraduate Program.

¹E. Bellingeri, L. Pellegrino, D. Marre, I. Pallecchi, and A. S. Siri, *J. Appl. Phys.* **94**, 5976 (2003).

²X. X. Xi, C. Doughty, A. Walkenhorst, S. N. Mao, Q. Li, and T. Venkatesan, *Appl. Phys. Lett.* **61**, 2353 (1992).

³K. Shimoyama, K. Kubo, T. Maeda, and K. Yamabe, *Jpn. J. Appl. Phys., Part 2* **40**, L463 (2001).

⁴S. Mochizuki, F. Fujishiro, and S. Minami, *J. Phys.: Condens. Matter* **17**, 923 (2005).

⁵D. A. Tenne, I. E. Gonenli, A. Soukiassian, D. G. Schlom, S. M. Nakhmanson, and K. M. Rabe, *Phys. Rev. B* **76**, 024303 (2007).

⁶C. Lee, J. Destry, and J. L. Brebner, *Phys. Rev. B* **11**, 2299 (1975).

- ⁷K. Szot, W. Speier, R. Carius, U. Zastrow, and W. Beyer, *Phys. Rev. Lett.* **88**, 075508 (2002).
- ⁸E. S. Kirkpatrick, K. A. Muller, and R. S. Rubins, *Phys. Rev.* **135**, A86 (1964).
- ⁹K. A. Muller, W. Berlinger, and R. S. Rubins, *Phys. Rev.* **186**, 361 (1969).
- ¹⁰R. A. Serway, W. Berlinger, K. A. Muller, and R. W. Collins, *Phys. Rev. B* **16**, 4761 (1977).
- ¹¹K. A. Muller and W. Berlinger, *J. Phys. C* **16**, 6861 (1983).
- ¹²K. A. Muller, *Helv. Phys. Acta* **31**, 173 (1958).
- ¹³B. W. Faughnan, *Phys. Rev. B* **4**, 3623 (1971).
- ¹⁴F. J. Morin and J. R. Oliver, *Phys. Rev. B* **8**, 5847 (1973).
- ¹⁵S. A. Basun, U. Bianchi, V. E. Bursian, A. A. Kaplyanskii, W. Kleemann, L. S. Sochava, and V. S. Vikhnin, *Proc. SPIE* **2706**, 73 (1996).
- ¹⁶R. Merkle and J. Maier, *Phys. Chem. Chem. Phys.* **5**, 2297 (2003).
- ¹⁷G. Koster, B. L. Kropman, G. J. H. M. Rijnders, D. H. A. Blank, and H. Rogalla, *Appl. Phys. Lett.* **73**, 2920 (1998).
- ¹⁸J. A. Weil, J. R. Bolton, and J. E. Wertz, *Electron Paramagnetic Resonance* (Wiley, New York, 1994).
- ¹⁹C. Lee, J. Yahla, and J. L. Brebner, *Phys. Rev. B* **3**, 2525 (1971).
- ²⁰O. N. Tufte and P. W. Chapman, *Phys. Rev.* **155**, 796 (1967).